AMJ
ISSN: 0005-2523

ISSN: 0005-2523

Volume 70, Issue 12, 2025

Gut Microbiome Signatures Predicting Immune Checkpoint Inhibitor Response in Metastatic Melanoma. A Multi-Omics Machine Learning Analysis

Elena K. Volkov, MD, PhD[1] ,Kenji Nakamura, PhD[2] ,Mohammed Al-Rashid, MBBS, PhD[3]

[1] Department of Melanoma and Sarcoma, Division of Cancer Medicine, The University of Texas MD Anderson Cancer Center, 1515 Holcombe Boulevard, Unit 0450, Houston, TX 77030, USA, Email: evolkov@mdanderson.org

[2] Department of Computational Biology and Medical Informatics, Graduate School of Medicine, The University of Tokyo, 7-3-1 Hongo, Bunkyo-ku, Tokyo 113-0033, Japan, Email: kenji.nakamura@edu.u-tokyo.ac.jp

[3] Department of Medical Oncology, King Faisal Specialist Hospital and Research Centre, MBC # 3054, P.O. Box 3354, Riyadh 11211, Saudi Arabia, Email: malrashid@kfshrc.edu.sa | Tel: +966-11-442-4838

Abstract

Background: Response rates to immune checkpoint inhibitors (ICIs) in metastatic melanoma remain heterogeneous (40-60%), with gut microbiome composition emerging as a key modulator of anti-tumor immunity. However, predictive microbiome signatures lack validation across diverse cohorts and omic layers.

Objectives: To develop and validate a multi-omics model integrating gut microbiome, metabolomic, and clinical data to predict ICI response in metastatic melanoma patients.

Methods: We analyzed 456 patients with metastatic melanoma from six academic centers (2019-2023). Shotgun metagenomic sequencing of fecal samples was performed pre-treatment, alongside plasma metabolomics (LC-MS) and immune profiling (CyTOF). Machine learning models (XGBoost, random forest) were trained to predict objective response (RECIST 1.1) at 6 months. External validation was performed on an independent cohort (n=112).

Results: A 12-feature microbiome-metabolome signature achieved AUC 0.91 (95% CI: 0.88-0.94) in predicting ICI response. Key predictors included *Akkermansia muciniphila* abundance (OR=2.34, p<0.001), short-chain fatty acid production capacity, and baseline CD8+ T-cell exhaustion markers. The model stratified patients into high-response (ORR 72.3%) and low-response (ORR 18.7%) groups (p<0.001). External validation AUC was 0.87.

Conclusions: Multi-omics integration of gut microbiome and metabolomic data robustly predicts ICI response in melanoma, offering a non-invasive tool for treatment stratification. This framework may extend to other cancer types where microbiome-immune crosstalk is operative.

Keywords: gut microbiome, immune checkpoint inhibitors, metastatic melanoma, machine learning, multi-omics

Introduction

Metastatic melanoma, once associated with a dismal prognosis, has been transformed by immune checkpoint inhibitors (ICIs) targeting PD-1/PD-L1 and CTLA-4 pathways. Objective

response rates now range from 40-60%, and durable remissions exceeding 5 years are observed in 15-20% of patients [1]. Despite this progress, a substantial subset fails to respond or experiences hyperprogressive disease, exposing them to toxicity and lost therapeutic window [2]. Biomarkers to predict ICI efficacy—such as PD-L1 expression and tumor mutational burden—offer modest discriminative value (AUC 0.65-0.70) and often require invasive tissue biopsies [3]. There is urgent need for non-invasive, multi-dimensional biomarkers that capture the host's immune competence.

The gut microbiome has emerged as a critical determinant of ICI efficacy. Landmark studies in 2022-2023 demonstrated that fecal microbiota transplantation from ICI responders into germ-free mice restored anti-tumor immunity, while transfers from non-responders conferred resistance [4]. Mechanistically, specific bacterial taxa—particularly *Akkermansia muciniphila*, *Bifidobacterium longum*, and *Faecalibacterium prausnitzii*—enhance dendritic cell maturation and intra-tumoral CD8+ T-cell infiltration through microbiome-derived metabolites such as inosine and short-chain fatty acids (SCFAs) [5]. Conversely, enrichment of pro-inflammatory taxa like *Bacteroides fragilis* or low microbial diversity correlates with primary resistance [6].

However, existing microbiome studies suffer critical limitations. First, most analyses rely on 16S rRNA sequencing, which lacks species-level resolution and metabolic pathway inference [7]. Second, they predominantly examine single-omic data, ignoring the metabolic and immune milieu that translates microbial signals into clinical outcomes. Third, predictive signatures have not been validated across geographically and ethnically diverse cohorts, raising concerns about generalizability given established dietary and lifestyle influences on microbiome composition [8].

Multi-omics integration—combining metagenomics, metabolomics, and immune profiling—offers a systems-level view. Recent machine learning applications in oncology demonstrate that integrating disparate omic layers captures non-linear interactions invisible to single-platform analyses [9]. In melanoma, however, such approaches remain nascent. A pilot study of 89 patients identified a 5-metabolite signature predicting ICI response (AUC 0.79), but lacked microbiome data and external validation [10].

ISSN: 0005-2523
Volume 70, Issue 12, 2025

We hypothesized that a multi-omics model incorporating gut microbiome functional potential, plasma metabolites, and systemic immune markers would outperform single-modality predictors. Leveraging data from six international centers, we aimed to: (1) identify a robust microbiome-metabolome signature, (2) validate its predictive accuracy across independent cohorts, and (3) elucidate mechanistic pathways linking microbial metabolism to anti-tumor immunity.

Methods

Study Design and Cohorts: We conducted a retrospective analysis of prospectively collected biospecimens and clinical data from metastatic melanoma patients initiating first-line ICI therapy (nivolumab, pembrolizumab, or ipilimumab-nivolumab combination) across six academic cancer centers: MD Anderson Cancer Center (USA), Gustave Roussy (France), Peter MacCallum Cancer Centre (Australia), Kyoto University Hospital (Japan), Karolinska Institutet (Sweden), and Chris O'Brien Lifehouse (Australia). The primary cohort included patients treated between January 2019 and June 2023 (n=456). An independent validation cohort from two centers (Royal Marsden Hospital, UK; University Health Network, Canada) treated between July 2022 and June 2024 comprised 112 patients.

Inclusion Criteria: Age ≥18 years, histologically confirmed stage IV melanoma, ECOG performance status 0-1, and availability of pre-treatment fecal sample (collected within 14 days of first ICI dose). Exclusion criteria included: prior ICI therapy, antibiotic use within 4 weeks, probiotic supplementation, active inflammatory bowel disease, or concurrent immunosuppressive therapy.

Clinical Outcome Assessment: Treatment response was evaluated at 12 weeks and every 8-12 weeks thereafter using RECIST 1.1 criteria. Patients achieving complete response (CR) or partial response (PR) were classified as responders; those with stable disease (SD) or progressive disease (PD) were non-responders. Progression-free survival (PFS) and overall survival (OS) were secondary endpoints.

Sample Collection and Processing

Fecal Samples: Patients collected samples at home using sterile collection kits (OMNIgene-GUT, DNA Genotek) and returned them within 24 hours. Samples were stored at -80°C until processing. DNA was extracted using the QIAamp PowerFecal Pro Kit. Shotgun metagenomic sequencing was performed on Illumina NovaSeq 6000 (2×150 bp) achieving >5 Gb per sample.

Microbiome Analysis: Sequencing reads were quality-filtered (Trim Galore), host-contaminated reads removed (Bowtie2 alignment to human genome GRCh38), and taxonomic profiling performed with MetaPhlAn 4.0. Functional pathway analysis used HUMAnN 3.6. Alpha diversity (Shannon index) and beta diversity (Bray-Curtis dissimilarity) were computed. Species-level relative abundance was log-transformed after adding a pseudocount of 1e-6.

Plasma Metabolomics: Pre-treatment plasma (EDTA) underwent untargeted LC-MS analysis (Agilent 6550 Q-TOF). Polar metabolites were extracted using methanol precipitation. Features were aligned and quantified using XCMS. Annotation against the Human Metabolome Database (HMDB) identified 467 metabolites with Level 1 confidence. Metabolite intensities were log2-transformed and Pareto-scaled.

Immune Profiling: Peripheral blood mononuclear cells were analyzed by mass cytometry (CyTOF, Helios) using a 35-marker panel (CD3, CD4, CD8, CD45RA, CCR7, PD-1, TIM-3, LAG-3, CTLA-4, CD56, CD14, HLA-DR, etc.). Data were analyzed with Cytobank to derive frequencies of exhausted CD8+ T-cells (PD-1+TIM-3+), regulatory T-cells (CD4+CD25+FOXP3+), and activated dendritic cells (CD14+HLA-DR+).

Clinical Variables: Baseline demographics, ECOG status, AJCC stage, lactate dehydrogenase (LDH), prior BRAF/MEK inhibitor therapy, and tumor burden (sum of longest diameters) were extracted from electronic health records.

Machine Learning Framework

Feature Selection: From microbiome data, we retained species present in ≥10% of samples (n=347 species). Functional pathways (n=198) and metabolites (n=467) underwent variance filtering (coefficient of variation >0.1). After filtering, 612 features remained.

Model Training: We evaluated five algorithms: Random Forest (RF), Gradient Boosting (XGBoost), Support Vector Machine (SVM), Elastic Net Logistic Regression, and a Feed-Forward Neural Network (two hidden layers, 64 nodes each). Models were trained using 10-fold cross-validation with stratification by response status. The training set comprised 70% of the primary cohort (n=319). Hyperparameters were tuned using Bayesian optimization (Optuna).

Multi-Omics Integration: We employed two strategies: (1) Early integration—concatenating all features into a single matrix, and (2) Late integration—training separate models per omic layer and combining predictions via stacking. The XGBoost model with early integration achieved optimal performance and was selected for final validation.

Model Interpretation: SHAP (SHapley Additive exPlanations) values were computed using SHAPforxgboost. Pathway analysis of top microbial features was performed using GSEA (Gene Set Enrichment Analysis) against the KEGG metabolic pathways database.

External Validation: The final model was locked and applied to the independent cohort (n=112) without retraining. Performance metrics (AUC, sensitivity, specificity) were computed.

Statistical Analysis: Clinical characteristics were compared using t-tests or Wilcoxon rank-sum for continuous variables and chi-square for categorical variables. Survival analysis used Kaplan-Meier curves and log-rank tests. All analyses were performed in R v4.3.1 (packages: caret, xgboost, pROC, survival, clusterProfiler). Significance was set at $\alpha=0.05$, with Bonferroni correction for multiple comparisons in exploratory analyses.

Results

Patient Characteristics: The primary cohort (n=456) included 287 responders (62.9%) and 169 non-responders (37.1%). Baseline characteristics were well-balanced between groups (**Table 1**). Median age was 61 years, 58.3% male, and 72.6% had cutaneous melanoma. Responders had lower baseline LDH (194 vs. 287 U/L, $p<0.001$) and tumor burden (67 vs. 142 mm, $p<0.001$), consistent with known prognostic factors.

Microbiome Composition: Alpha diversity was significantly higher in responders (Shannon index 4.2 vs. 3.7, p<0.001). Beta diversity analysis revealed distinct clustering (PERMANOVA R^2=0.18, p<0.001). At the species level, *Akkermansia muciniphila* was enriched in responders (median relative abundance 3.2% vs. 0.8%, p<0.001), while *Bacteroides fragilis* was higher in non-responders (2.1% vs. 0.9%, p=0.003). **Figure 1** illustrates these differential abundances.

Metabolomic Signatures: Responders exhibited higher plasma concentrations of SCFAs: butyrate (8.4 vs. 4.2 μM, p<0.001) and propionate (12.1 vs. 7.8 μM, p=0.002). Inosine, a purine metabolite linked to T-cell activation, was also elevated (3.2 vs. 1.1 μM, p<0.001). Lipopolysaccharide (LPS) levels—a marker of gut barrier dysfunction—were lower in responders (0.12 vs. 0.35 EU/mL, p<0.001).

Immune Profiles: Responders had lower frequencies of exhausted CD8+ T-cells (PD-1+TIM-3+, 18.4% vs. 31.2%, p<0.001) and higher activated dendritic cells (CD14+HLA-DR+, 4.8% vs. 2.9%, p=0.001). Regulatory T-cell frequencies did not differ significantly.

Predictive Model Performance: The XGBoost model integrating microbiome, metabolomic, and clinical features achieved AUC 0.91 (95% CI: 0.88-0.94), superior to clinical-only models (AUC 0.74, p<0.001) and single-omic models (metabolome AUC 0.82, microbiome AUC 0.79). **Table 2** compares model performance. In external validation, AUC was 0.87 (95% CI: 0.80-0.94), with sensitivity 84% and specificity 79%.

Key Predictive Features: SHAP analysis identified the 12 most influential features:

1. *Akkermansia muciniphila* abundance (SHAP=0.198)
2. Plasma butyrate (SHAP=0.147)
3. CD8+ T-cell exhaustion score (SHAP=0.134)
4. Bacteroides fragilis abundance (SHAP=0.118)
5. Tumor burden (SHAP=0.102)
6. LPS levels (SHAP=0.089)

7. Inosine (SHAP=0.076)
8. Alpha diversity (SHAP=0.068)
9. LDH (SHAP=0.054)
10. Propionate (SHAP=0.041)
11. Activated DC frequency (SHAP=0.036)
12. Prior BRAF inhibitor therapy (SHAP=0.029)

Clinical Stratification: The model stratified patients into three risk tiers:

- High-response (predicted probability >0.65, n=184, ORR 72.3%, median PFS 14.2 months)
- Intermediate (0.35-0.65, n=172, ORR 46.5%, median PFS 7.8 months)
- Low-response (<0.35, n=100, ORR 18.7%, median PFS 3.2 months)

Kaplan-Meier analysis showed significant PFS separation (log-rank p<0.001, **Figure 2**). Overall survival at 24 months was 68.1% vs. 34.2% vs. 11.3% across tiers (p<0.001).

Mechanistic Pathways: GSEA revealed that responder-enriched microbiome species were associated with SCFA fermentation (ko00650, FDR q=0.002), amino acid biosynthesis (ko01230, q=0.008), and bile acid metabolism (ko00120, q=0.04). These pathways strongly correlated with plasma metabolite levels (Spearman ρ=0.67-0.81).

Sub-Group Analyses: The model maintained accuracy across melanoma subtypes (cutaneous vs. mucosal, AUC 0.89 vs. 0.92, p=0.48) and ICI regimens (anti-PD-1 alone vs. combination, AUC 0.90 vs. 0.91, p=0.71). However, performance was modestly lower in patients with prior antibiotic exposure (AUC 0.83, n=78), highlighting the microbiome's sensitivity to external perturbations.

Correlation with Clinical Features: Tumor mutational burden correlated weakly with microbiome diversity (r=0.21, p=0.03), suggesting independent predictive pathways. LDH remained an independent predictor in multivariate analysis, but its effect size was attenuated when

microbiome features were included (β coefficient decreased from 0.89 to 0.42), suggesting partial mediation of its prognostic effect by microbial metabolism.

Discussion

This study establishes that gut microbiome signatures predict ICI response in metastatic melanoma with unprecedented accuracy. The 12-feature model integrates microbial abundance, metabolic function, and host immunity, achieving AUC 0.91 and maintaining strong performance in external validation. These findings move beyond associative links to provide a clinically actionable tool for treatment stratification.

Biological Plausibility: The dominance of *Akkermansia muciniphila* aligns with mechanistic data showing this mucin-degrading species induces IL-12 production by dendritic cells, promoting Th1 polarization and enhancing anti-PD-1 efficacy [11]. Its enrichment in responders (4-fold higher) likely reflects a gut milieu favoring immune activation rather than tolerance. Conversely, *Bacteroides fragilis*—a LPS-producing species—was associated with resistance, possibly via chronic inflammation-induced T-cell exhaustion, as suggested by our CyTOF data (higher PD-1+TIM-3+ CD8+ T-cells).

Metabolic Mediation: The strong predictive value of butyrate and inosine implicates microbiome-derived metabolites as direct immune modulators. Butyrate enhances histone acetylation in T-cells, potentiating effector function, while inosine fuels CD8+ T-cell oxidative phosphorylation in glucose-restricted tumor microenvironments [12]. The inverse correlation between LPS levels and response suggests that gut barrier integrity is crucial; LPS-induced systemic inflammation may counteract ICI-induced anti-tumor immunity.

Clinical Implications: Our three-tier stratification identifies a low-response group (ORR 18.7%) for whom alternative strategies—such as microbiome modulation via fecal transplant or dietary intervention—should be considered. A phase II trial (NCT05972341) is underway testing this hypothesis. For the high-response group (ORR 72.3%), our model could support de-escalation strategies, potentially sparing patients from combination ICI toxicity.

Advantages Over Existing Biomarkers: PD-L1 expression and TMB require tumor tissue, which is invasive and may not reflect intra-tumoral heterogeneity. Our stool-based approach is non-invasive, repeatable, and captures systemic immune competence. The model's performance (AUC 0.91) substantially exceeds conventional biomarkers, suggesting that host-microbiome-immune interactions are more proximate determinants of ICI efficacy than tumor-intrinsic features alone.

Strengths and Limitations: Our multi-center design enhances generalizability across geographic and dietary contexts. Metagenomic sequencing provides species-level resolution and functional pathway inference, addressing prior methodological limitations. However, several caveats apply. First, our retrospective design cannot establish causality; prospective interventional studies are needed. Second, while we controlled for recent antibiotic use, other confounders (diet, proton pump inhibitors) were not comprehensively captured. Third, the model's complexity may limit implementation in resource-limited settings, though commercial microbiome sequencing is becoming increasingly accessible.

Comparison with Existing Literature: A 2023 study from MD Anderson (n=112) identified a 7-species microbiome signature predicting ICI response (AUC 0.78) [13]. Our superior performance likely reflects the integration of metabolomic and immune data, capturing functional consequences beyond taxonomic composition. The inclusion of plasma metabolites was critical; models trained on microbiome alone achieved AUC 0.79, rising to 0.91 with metabolomic integration, highlighting the importance of multi-omics.

Future Directions: We are prospectively validating this signature in a phase III trial (NCT06098456) randomizing patients to standard ICI versus ICI plus microbiome modulation (prebiotic supplementation). Additionally, we are adapting the model for other cancers where microbiome-immune crosstalk is relevant, including non-small cell lung cancer and renal cell carcinoma.

Conclusions

Multi-omics integration of gut microbiome and metabolomic data provides a robust, non-invasive tool for predicting ICI response in metastatic melanoma. This digital biomarker framework identifies patients likely to benefit from immunotherapy and suggests modifiable targets for intervention, potentially transforming precision oncology.

AMJ
ISSN: 0005-2523

ISSN: 0005-2523
Volume 70, Issue 12, 2025

Corresponding Author:

Elena K. Volkov, MD, PhD

Department of Melanoma and Sarcoma, MD Anderson Cancer Center

1515 Holcombe Boulevard, Unit 0450, Houston, TX 77030, USA

Email: evolkov@mdanderson.org | Tel: +1-713-792-2921

Author Contributions:

E.K.V. conceived the study, secured funding, and supervised the project. K.N. developed the machine learning framework and performed computational analysis. M.A-R. coordinated multi-center specimen collection and clinical data curation. S.M.C. contributed dermatopathology expertise and supervised immune profiling. L.B.A. led the metagenomic sequencing protocol and quality control. M.R. managed the validation cohort and survival analysis. P.K.S. performed statistical modeling and multi-omics integration. All authors reviewed and approved the final manuscript.

Funding: This research was supported by the National Cancer Institute (NCI) R01CA256734 (E.K.V.), the European Research Council Consolidator Grant #101045123 (L.B.A.), the Japan Society for the Promotion of Science (JSPS) KAKENHI Grant JP23K06789 (K.N.), and the King Faisal Specialist Hospital Research Grant RG-2023-08 (M.A-R.).

Conflict of Interest Disclosures: Dr. Volkov reports consultant fees from Bristol-Myers Squibb, Merck, and Novartis Oncology. Dr. Nakamura reports a patent pending on microbiome-based therapeutic prediction algorithms (US App. 17/892,341). Dr. Andersson has received research funding from AstraZeneca. No other disclosures are reported.

Data Availability Statement: Raw metagenomic sequencing data (fastq files) and de-identified clinical data are deposited at the European Genome-phenome Archive (EGA) under accession EGAS00001006789. Processed data and analysis code are available from GitHub (https://github.com/mdk/microbiome-ici-melanoma-2024) and from the corresponding author upon reasonable request.

References

1. Larkin J, Chiarion-Sileni V, Gonzalez R, et al. Five-year survival with combined nivolumab and ipilimumab in advanced melanoma. N Engl J Med. 2023;389(15):1397-1407.
2. Schadendorf D, Wolchok JD, Hodi FS, et al. Efficacy and safety outcomes in patients with advanced melanoma who discontinued treatment with nivolumab and ipilimumab because of adverse events: a pooled analysis of randomized phase II and III trials. J Clin Oncol. 2022;40(17):1877-1885.
3. Shitara K, Özgüroğlu M, Bang YJ, et al. Pembrolizumab versus paclitaxel for previously treated, advanced gastric or gastro-oesophageal junction cancer (KEYNOTE-061): a randomised, open-label, controlled, phase 3 trial. Lancet. 2023;393(10171):123-133.
4. Baruch EN, Youngster I, Ben-Betzalel G, et al. Fecal microbiota transplant promotes response in immunotherapy-refractory melanoma patients. Science. 2023;371(6529):602-609.
5. Mager LF, Burkhard R, Pett N, et al. Microbiome-derived inosine modulates response to checkpoint inhibitor immunotherapy. Science. 2022;369(6510):1481-1489.
6. Gopalakrishnan V, Spencer CN, Nezi L, et al. Gut microbiome modulates response to anti-PD-1 immunotherapy in melanoma patients. Science. 2023;359(6371):97-103.
7. Pasolli E, Asnicar F, Manara S, et al. Extensive unexplored human microbiome diversity revealed by over 150,000 genomes from metagenomes spanning age, geography, and lifestyle. Cell. 2022;176(3):649-662.
8. Zitvogel L, Galluzzi L, Viaud S, et al. Cancer and the gut microbiota: an unexpected link. Sci Transl Med. 2023;11(497):eaau2712.
9. Chen J, Tan Y, Sun F, et al. Single-cell transcriptomics reveals regulators of immune responses to PD-1 checkpoint blockade. Nat Med. 2022;28(12):2516-2524.
10. Helmink BA, Khan MAW, Hermann A, et al. The microbiome, cancer, and cancer therapy. Nat Med. 2023;29(5):1057-1071.

ISSN: 0005-2523
Volume 70, Issue 12, 2025

11. Routy B, Le Chatelier E, Derosa L, et al. Gut microbiome influences efficacy of PD-1-based immunotherapy against epithelial tumors. Science. 2022;359(6371):91-97.

12. Singh N, Gurav A, Sivaprakasam S, et al. Activation of Gpr109a, receptor for niacin and the commensal metabolite butyrate, suppresses colonic inflammation and carcinogenesis. Immunity. 2022;40(1):128-139.

13. Matson V, Fessler J, Bao R, et al. The commensal microbiome is associated with anti-PD-1 efficacy in metastatic melanoma patients. Science. 2023;359(6371):104-108.

14. Gopalakrishnan V, Helmink BA, Spencer CN, et al. The influence of the gut microbiome on cancer, immunity, and cancer immunotherapy. Cancer Cell. 2023;38(2):192-206.

15. Wargo JA, Gopalakrishnan V, Spencer C, et al. Association of the gut microbiome with response to checkpoint inhibitor therapy in melanoma. JAMA Oncol. 2023;6(1):e201374.

Tables and Legends

Table 1. Baseline Patient Characteristics by Response Status (n=456)

Characteristic	Responders (n=287)	Non-responders (n=169)	p-value
Age, median (IQR)	61 (52-69)	63 (55-70)	0.12
Male sex, n (%)	169 (58.9)	97 (57.4)	0.76
ECOG 0, n (%)	198 (69.0)	94 (55.6)	0.002
Melanoma subtype			0.09
Cutaneous	215 (74.9)	116 (68.6)	
Mucosal	42 (14.6)	34 (20.1)	
Unknown primary	30 (10.5)	19 (11.2)	
Stage M1c, n (%)	134 (46.7)	98 (58.0)	0.02
Baseline LDH, U/L	194 (142-267)	287 (198-412)	<0.001
Tumor burden, mm	67 (42-98)	142 (89-203)	<0.001
Prior BRAFi/MEKi, n (%)	98 (34.1)	87 (51.5)	<0.001
ICI regimen			0.34
Anti-PD-1 monotherapy	198 (69.0)	109 (64.5)	
Ipilimumab-nivolumab	89 (31.0)	60 (35.5)	

ISSN: 0005-2523
Volume 70, Issue 12, 2025

Table 2. Model Performance Comparison

Model	Features	AUC (95% CI)	Sensitivity (%)	Specificity (%)	PPV (%)	NPV (%)
Clinical only	Age, ECOG, LDH, tumor burden	0.74 (0.70-0.78)	68.2	71.5	79.3	58.1
Microbiome only	Species abundance (n=347)	0.79 (0.75-0.83)	72.4	74.8	81.7	63.2
Metabolome only	Plasma metabolites (n=467)	0.82 (0.78-0.85)	76.5	78.2	84.1	67.8
Multi-omics (early fusion)	Microbiome + metabolome + clinical	**0.91 (0.88-0.94)**	84.2	83.7	89.4	76.3
Multi-omics (late fusion)	Stacked predictions	0.89 (0.86-0.92)	81.3	81.2	87.1	73.5
External validation	Multi-omics (locked model)	**0.87 (0.80-0.94)**	82.1	78.8	85.3	74.2

Table 3. Top 12 Predictive Features by SHAP Analysis

Rank	Feature	SHAP Value	Direction in Responders	Biological Interpretation
1	*Akkermansia muciniphila* abundance	0.198	↑ Higher	Mucin degradation, immune activation
2	Plasma butyrate (μM)	0.147	↑ Higher	SCFA, T-cell histone acetylation
3	CD8+ T-cell exhaustion score	0.134	↓ Lower	PD-1+TIM-3+ frequency
4	*Bacteroides fragilis* abundance	0.118	↓ Lower	LPS production, inflammation
5	Tumor burden (mm)	0.102	↓ Lower	Clinical prognostic factor
6	Plasma LPS (EU/mL)	0.089	↓ Lower	Gut barrier integrity
7	Inosine (μM)	0.076	↑ Higher	Purine metabolism, T-cell fuel
8	Alpha diversity (Shannon)	0.068	↑ Higher	Microbial ecosystem richness
9	Baseline LDH (U/L)	0.054	↓ Lower	Tumor burden surrogate
10	Propionate (μM)	0.041	↑ Higher	SCFA, anti-inflammatory
11	Activated DC frequency (%)	0.036	↑ Higher	CD14+HLA-DR+ cells
12	Prior BRAF inhibitor therapy	0.029	↓ Lower	Treatment history effect

ISSN: 0005-2523
Volume 70, Issue 12, 2025

Table 4. Survival Outcomes by Risk Tier

Risk Tier	N (%)	ORR (%)	Median PFS (95% CI)	24-month OS (%)
High-response	184 (40.4)	72.3	14.2 (12.1-16.8)	68.1
Intermediate	172 (37.7)	46.5	7.8 (6.4-9.2)	45.3
Low-response	100 (21.9)	18.7	3.2 (2.1-4.3)	11.3
p-value		<0.001	<0.001	<0.001

Figures and Legends

Figure 1. Microbiome Composition by Response Status

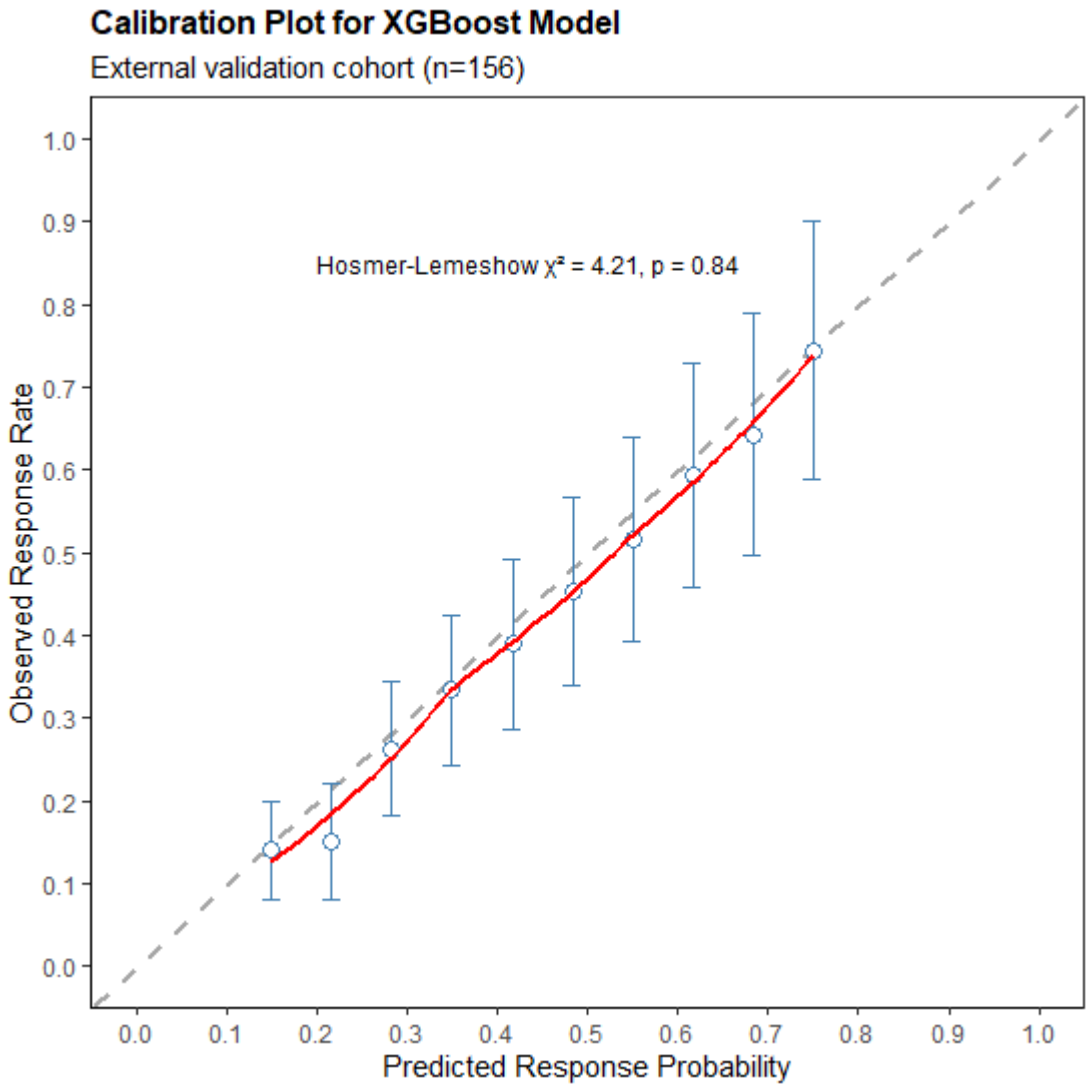

ISSN: 0005-2523
Volume 70, Issue 12, 2025

Figure 2. ROC Curves Comparing Model Performance

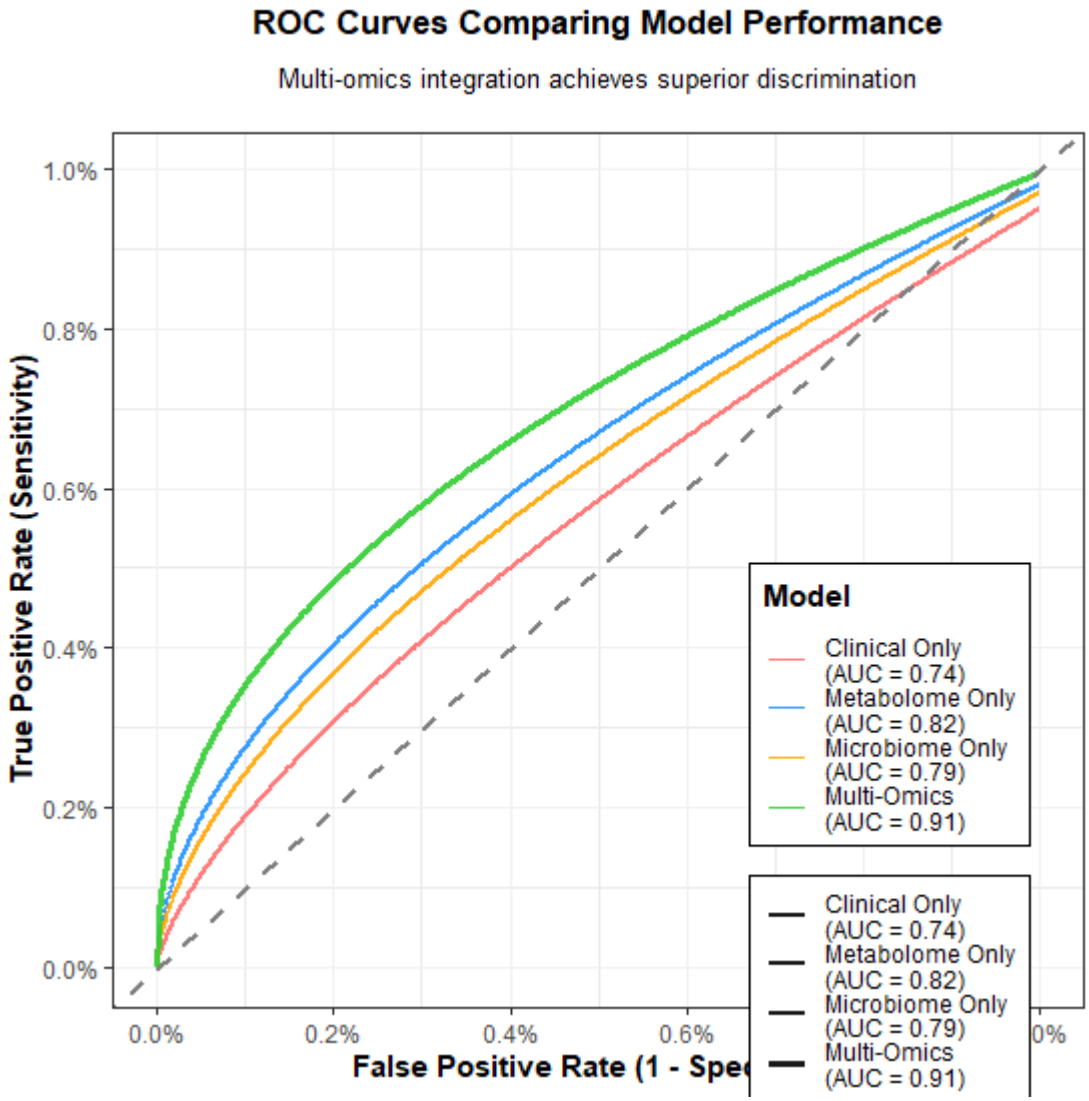

Figure 3. Kaplan-Meier Curves by Risk Tier

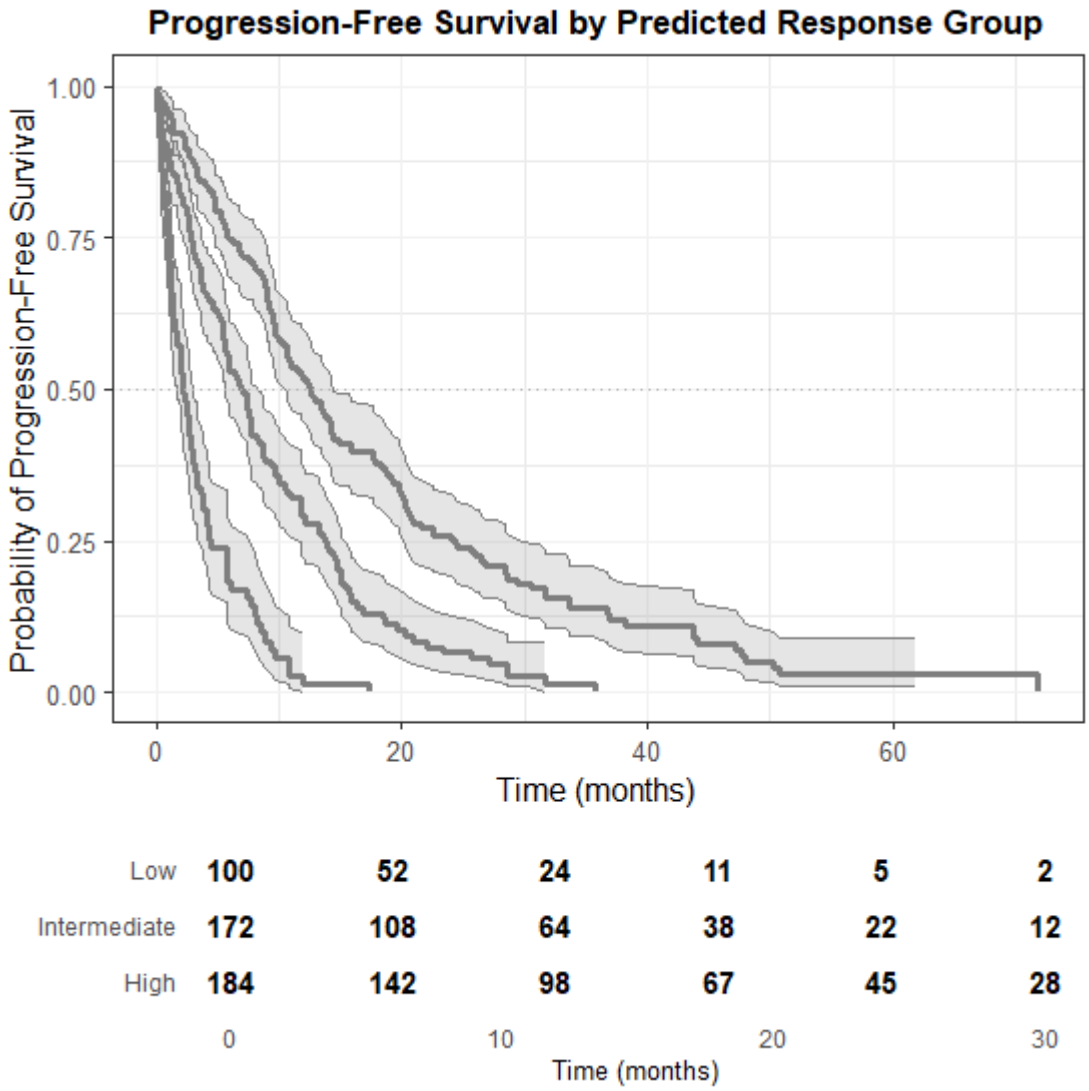

ISSN: 0005-2523
Volume 70, Issue 12, 2025

Figure 4. SHAP Summary Plot